DOI: https://doi.org/10.37434/tpwj2024.04.02

COMPUTATIONAL EVALUATION OF THE INFLUENCE OF THE THICKNESS OF WELDED JOINTS OF AMg6 ALLOY ON THEIR STRESS-STRAIN STATE AFTER ELECTRODYNAMIC TREATMENT IN THE PROCESS OF WELDING

L.M. Lobanov[1], **M.O. Pashchyn**[1], **O.L. Mikhodui**[1], **N.L. Todorovych**[1], **Yu.M. Sydorenko**[2], **P.R. Ustymenko**[2]

[1]E.O. Paton Electric Welding Institute of the NASU
11 Kazymyr Malevych Str., 03150, Kyiv, Ukraine
[2]National Technical University of Ukraine "Igor Sikorsky Kyiv Polytechnic Institute"
37 Prospect Beresteiskyi (former Peremohy), 03056, Kyiv, Ukraine

ABSTRACT

A calculated evaluation of the efficiency of electrodynamic treatment (EDT) effect on the stress state of butt-welded joints of plates of aluminium AMg6 alloy with an increase in their thickness δ was carried out. Mathematical modelling of the kinetics and residual stress states of butt-welded joints δ = 2, 4 and 8 mm was carried out as a result of their EDT at different values of temperature T of the plates, at which the treatment was performed. The value of the vertical velocity V_0 of the electrode-indenter (EDT tool) was taken as V_0 = 5 m/s, which corresponds to the modern electrophysical characteristics of the equipment for EDT. The values of T were set reflecting the conditions of EDT after welding (T = 20°C) and during fusion welding (T = 150 and 300 °C). The problem was solved in a three-dimensional formulation using the ANSYS softare. The conditions for the formation of stresses in the plates at EDT after and during welding were determined by the mechanical characteristics of AMg6 alloy at temperatures T = 20, 150, and 300 °C without taking cooling into account. The results of the computation of residual stresses in welded joints are presented. It is shown that at a value of T = 150 °C, EDT provides the most optimal residual stress states of the plates in the entire experimental range of δ. It was proved that EDT in the welding process (at T = 150 °C) is more efficient compared to EDT of metal after cooling (T = 20 °C). It was established that at EDT of welded joints δ = 2–4 mm, residual compressive stresses are formed over the entire thickness of the plates, the values of which are close to the yield strength of AMg6 alloy. At EDT of welded joints δ = 8 mm, residual compressive stresses are formed on the outer surface of the plates, and on the back side — tensile ones.

KEYWORDS: electrodynamic treatment, residual welding stresses, aluminium alloy, electric current pulse, shock interaction, finite element model, electrode-indenter, theory of elastic-plastic flow, fusion welding

INTRODUCTION

Residual stresses have a negative impact on the life and corrosion resistance of welded structures of aluminium-based alloys, thereby reducing their service life. In the world practice, an increase in the volumes of manufacturing of such structures is observed, which replace high-strength steel products. Considering the abovementioned, the problem of reducing residual tensile stresses or forming compression stresses in welded joints of aluminium-based alloys is relevant. Traditional technologies for control of residual stress state (RSS) require the use of metal-intensive tooling and/or significant energy consumption and do not always meet the requirements of modern engineering practice [1, 2], which requires innovative energy-saving approaches to production.

RESEARCH RELEVANCE

Electrodynamic treatment (EDT) of welded joints with electric current pulses is an innovative approach to controlling RSS of welded structures based on the use of pulsed electromagnetic fields and their derivatives [3–6].

It has been proved that preheating of the electric pulse effect zone to a temperature T stimulates RSS relaxation mechanisms [7]. This contributes to the development of technologies for the use of EDT in combination with the welding process. It has been experimentally proved that the implementation of EDT at elevated T during welding contributes to more intensive RSS relaxation as a result of EDT compared to the treatment of weld metal at room T [8].

However, the electrophysical characteristics of the existing EDT equipment provide the value of the stored energy E_C (the value of E_C is the defining characteristic of EDT efficiency) of the capacitive storage C, which does not exceed 1.0 kJ. This predetermines the evaluation of the boundary capabilities of EDT application as a means of effective influence on RSS of welded structures. As is known from the results of previous experimental studies, the effectiveness of

EDT decreases with an increase in the thickness δ of the metal to be treated [9]. Until now, no theoretical evaluation of the effect of δ of welded joints on EDT efficiency has been carried out, including when treating metal at different T values, to which the metal is heated during welding. The results of such studies allow determining the maximum boundary δ of welded joints within which EDT is an effective RSS regulator with the existing capabilities of EDT equipment, i.e., at the condition $E_C \leq 1$ kJ, which corresponds to the kinetic energy of the electrode-indenter at a velocity of up to 5 m/s. The way to solve the problem is the mathematical modelling, first of all, of the dynamic (shock) component of EDT to determine the effect of different δ of welded joints on RSS after their EDT during and after welding. This should facilitate the optimization of the EDT technology by determining the boundary capabilities of its application for effective RSS control of welded joints.

The aim of the study is the computational evaluation of the influence of the thickness of welded joints on their RSS as a result of treatment of metal by shock EDT component after and during welding (at elevated temperatures).

PROCEDURE AND COMPUTATIONAL SCHEME OF THE PROBLEM

The object of research is the process of numerical computation of SSS of model welded joints as a result of shock treatment as a component of EDT under conditions of elevated temperatures, which was performed in a finite element formulation using the ANSYS/AUTODYN software [10] in an explicit form. A three-dimensional prismatic finite element SOLID 164 was used to build the finite element mesh (FEM) of the problem, and the modelling was performed with the use of a moving FEM, that was rigidly connected with the medium and deformed together with it. The computational scheme and boundary conditions of the problem regarding the process of shock interaction of the electrode-indenter with a plate, described in [8], are shown in Figure 1. The presence of the geometric symmetry of the dynamically interacting electrode *1* and plate *2* allows considering only their fourth part in the computational scheme with the limitation of bodies' displacements on the symmetry planes.

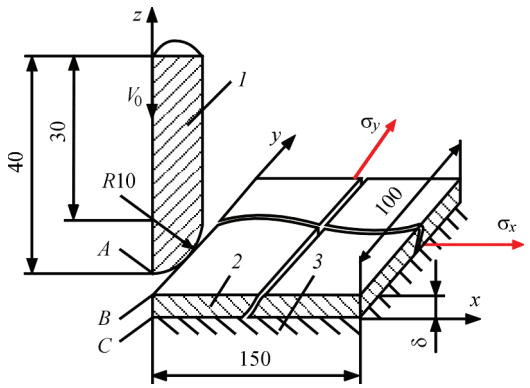

Figure 1. Computational diagram of the process of dynamic loading of the plate at EDT: *1* — electrode-indenter; *2* — treated specimen; *3* — absolutely rigid base; *A* — point on the outer surface of the electrode-indenter; *B* — point on the outer surface of the plate; *C* — point on the back surface of the plate; V_0 — velocity of the electrode-indenter movement [8]; *x*, *y*, *z* — coordinate axes

As the subject of the research, a model of a butt-welded joint of AMg6 alloy of the Al–Mg alloying system in the form of a plate preliminary stressed by uniform uniaxial tension was used. Residual welding stresses in the plate plane were modelled by setting the T value of the longitudinal tensile stress component σ_x (along the *x*-axis in Figure 1). Since the effect of EDT on the stress state of the treated plate is quite local in size, for example, not more than 10–15 mm, it can be assumed that in the zone of residual tensile stresses at EDT, these stresses can be taken as constant. The applied computational scheme is simplified, it does not reproduce the actual distribution of residual stresses in the welded joint, but requires the minimal computation time. Based on the results of comparing σ_x in the weld centre (in the contact interaction zone) after EDT at different T values, it is possible to select the temperature treatment mode that provides optimal residual stresses. The scheme for computation of the real stress distributions in the cross-section of a welded joint, taking into account the active zone – tension and reactive – compression zone, will be implemented in further studies.

In the mathematical formulation, the behaviour of the materials of the plate (aluminium AMg6 alloy) and the electrode-indenter (M1 copper) under the action of an external pulse load was described using an ideal elastic-plastic material model. This model in the materials library of the ANSYS/AUTODYN software is called PLASTIC-KINEMATIC [10]. The contact interaction was frictionless.

The interaction of the electrode-indenter with the plates of 300×200 mm and a thickness δ = 2, 4 and 8 mm was considered, which according to the accepted classification belong to thin-sheet structures [11].

The effect of temperature without taking the cooling of the model welded joint into account was described by changing such mechanical characteristics as modulus of elasticity E and yield strength σ_y of AMg6 alloy at temperatures T = 150 and 300 °C, where the choice of T values was justified in [8]. The modeling was also performed for T = 20 °C to compare the efficiency of EDT after and during welding. The values of residual welding stress component σ_x were respectively assumed to be equal to σ_y of AMg6 alloy at T = 20, 150, and 300 °C. The mechanical

Table 1. Mechanical characteristics of structural elements of the EDT model of AMg6 alloy in the welding process

Number	Structural element of the model	Material	Density ρ, kg/m³	Poisson's ratio μ	*T*, °C	Modulus of elasticity *E*, GPa	Yield strength σ_y, MPa	Relative elongation δ, %
1	Plate of 300×200×2–8 mm	AMg6	2640	0.34	20	71	150	22
2					150	60	120	40
3					300	55	50	55
4	Electrode with a diameter of 15 mm	M1	8940	0.35	20	128	300	6

characteristics of metal materials used in the modelling at T = 20, 150, and 300 °C are given in Table 1.

The set T values correspond to the location of the electrode-indenter along the weld line at a distance L_{EDT} behind the welding heat source (Figure 2).

According to the results of previous experimental studies, it was found that the electrode-indenter obtained a value of V_0 = 5 m/s (at the condition E_C = 1 kJ), and its temperature during welding did not exceed 20 °C [8]. Therefore, the properties of the electrode-indenter during its contact interaction with the plate were set exclusively for T = 20 °C (Table 1).

MODELLING RESULTS AND THEIR DISCUSSION

As is known, σ_x component has a much greater influence on RSS of welded joints compared to σ_y [11]. As a result of modelling, the axonometric surfaces of the distribution of σ_x stress component (instantaneous stresses) across the metal thickness at the moment of completion of the contact interaction at T = 20, 150 and 300 °C of the electrode-indenter with a plate δ = 2 mm (Figure 3), δ = 4 mm (Figure 4) and δ = 8 mm (Figure 5) along the shock line (SL) at the points *B* and *C* (Figure 1), as well as on the *X* axis at a distance of 5 mm (Figure 3, *a*) from SL to evaluate the stress distribution along the center line of the weld.

Analysing the results of Figures 3–5 in general, it should be noted that after EDT at T = 150 and 300 °C, stresses are formed in the plates that slightly exceed the value of $\sigma_y = f(T)$ (Table 1). However, the mod-

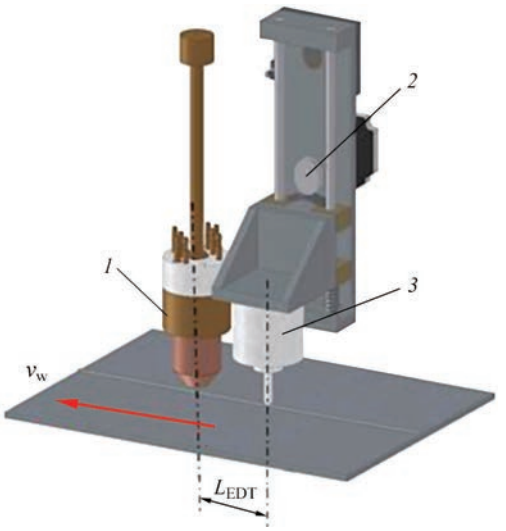

Figure 2. Scheme of EDT in the welding process, where V_w is the welding direction; *1* — welding torch; *2* — system for dynamic loading of EDT electrode; *3* — electrode device for EDT; L_{EDT} — distance between the axes of the electrodes for welding and EDT [8]

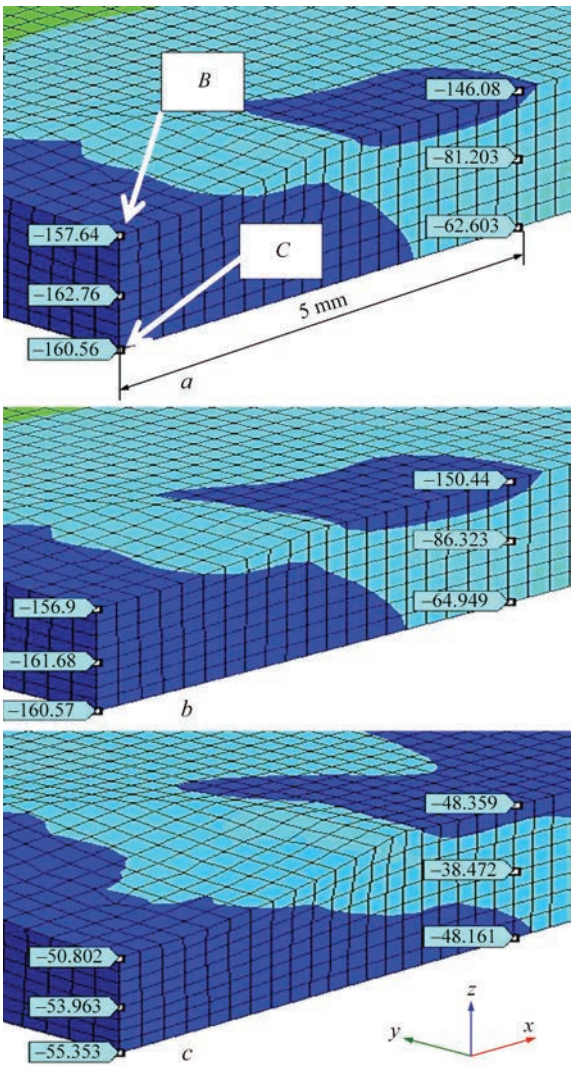

Figure 3. Instantaneous patterns of the distribution of values (MPa) of stress σ_x components in the plate of AMg6 alloy δ = 2 mm at the moment of completion of the EDT action along the shock line (SL) between the points *B* and *C* (Figure 2) and at a distance of 5 mm from the line *B*–*C*: *a* — σ_x at T = 20 °C; *b* — σ_x at T = 150 °C; *c* — σ_x at T = 300 °C

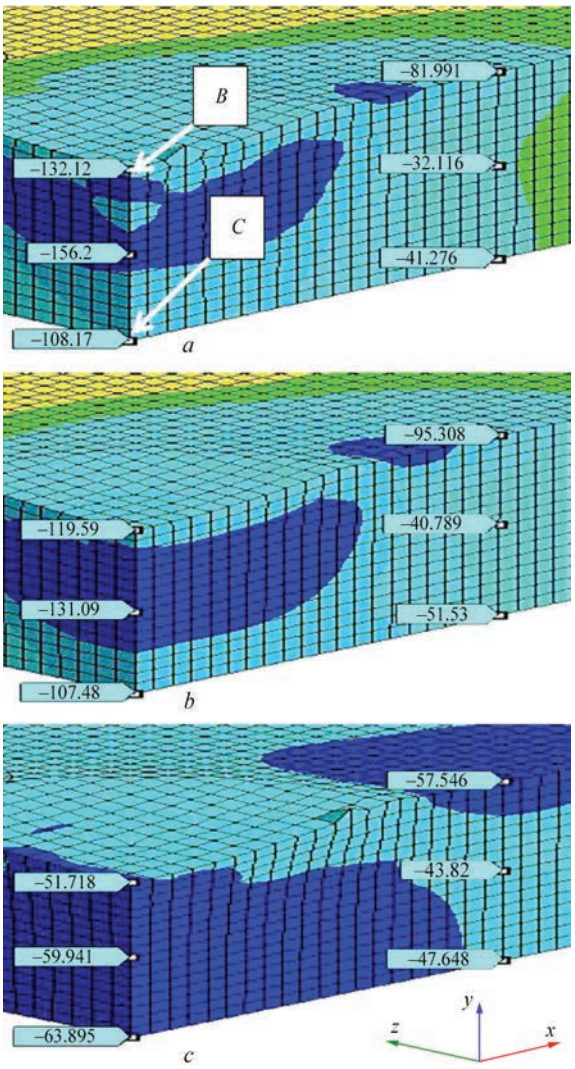

Figure 4. Instantaneous patterns of the calculated distribution of values (MPa) of stress σ_x components in the plate of AMg6 alloy δ = 4 mm at the moment of completion of the EDT action along the shock line (SL) between the points *B* and *C* and at a distance of 5 mm from the line *B*–*C*: *a* — σ_x at *T* = 20 °C; *b* — σ_x at *T* = 150 °C; *c* — σ_x at *T* = 300 °C

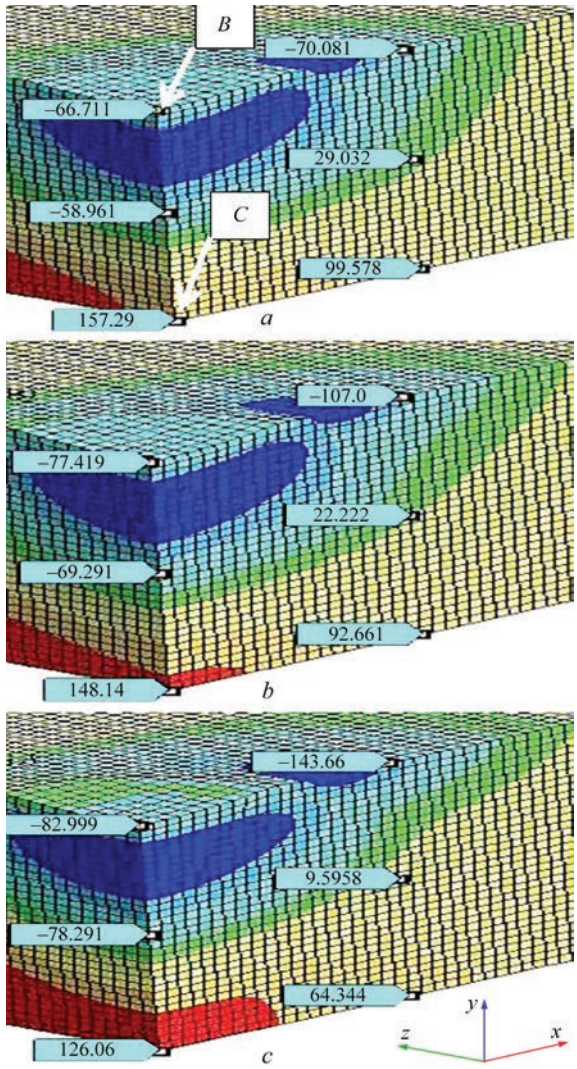

Figure 5. Instantaneous patterns of the calculated distribution of values (MPa) of stress σ_x, σ_y components in the plate of AMg6 alloy δ = 8 mm at the moment of completion of the EDT action along the line between the points *B* and *C* (Figure 2) and at a distance of 5 mm from the line *B*–*C*: *a* — σ_x at *T* = 20 °C; *b* — σ_x at *T* = 150 °C; *c* — σ_x at *T* = 300 °C

elling results allow (in terms of quality) comparing RSS of plates δ = 2–8 mm after EDT at different *T* and determining the optimal *T* value, at which the highest efficiency of EDT action on RSS of welded joints is achieved. The dominance of instantaneous compression σ_x stresses along SL in the entire considered range of δ and T can be seen. At a distance of 5 mm from SL, the pattern is slightly different. Thus, if for σ_x components in the range of δ = 2–4 mm at all T values, compression stresses dominate, then for δ = 8 mm, a change in the sign of stresses across the thickness of the plate from compression at the point *B* to tension at the point *C* is characteristic.

Figure 3 shows the results of computation of the instantaneous distributions of σ_x in the plates δ = 2 mm. It can be seen that along SL, σ_x components are exclusively compression stresses on the contact (point *B*) and back (point *C*) surfaces of the plates. The values of stresses along SL reach $\sigma_y = f(T)$ for AMg6 alloy at *T* = 20 °C (Figure 3, *a*) and 300 °C (Figure 3, *c*) and grow to $1.3\sigma_y$ at 150 °C (Figure 3, *b*). At a distance of 5 mm from SL, the compression σ_x values decrease from σ_y on the outer surface to $0.4\sigma_y$ on the back one at *T* = 20 °C (Figure 3, *a*) from 1.25 to $0.5\sigma_y$ at *T* = 150 °C (Figure 3, *b*) and are close to σ_y at 300 °C on both surfaces (Figure 3, *c*).

Comparing the instantaneous distributions of σ_x component at *T* = 20, 150 and 300 °C, which is dominant during the formation of residual welding stresses, it should be noted that the optimal temperature for EDT is 150 °C, at which the maximum level of compression (instantaneous) stresses is achieved at the moment of completion of contact interaction.

Figure 4 shows the results of computation of the instantaneous distributions of σ_x in the plates δ = 4 mm. It is possible to see some differences in stress distri-

butions from the previous results (δ = 2 mm), which are associated with an increase in the thickness of the treated plates. Thus, along SL and at a distance of 5 mm from it, the values of σ_x compression are generally lower than at δ = 2 mm.

The components of compression σ_x along SL (from the point *B* to the point *C*) reach the values respectively from $0.9\sigma_y$ to $0.7\sigma_y$ for AMg6 alloy at *T* = 20 °C (Figure 4, *a*), $1.1\sigma_y$ at 150 °C (Figure 4, *c*, *d*), i.e., lower than for δ = 2 mm. At *T* = 300 °C, the distributions of σ_x compression are close to σ_y (Figure 4, *e*, *f*), as well as for the plates δ = 2 mm. Even on the back surface, the values of σ_x compression grow to $1.2\sigma_y$. Comparing the values of σ_x stresses at *T* = 20 and 150 °C (Figure 4, *a*, *b*), it is possible to see that, as for the plates δ = 2 mm, heating to 150 ° C contributes to higher instantaneous stresses compared to EDT at *T* = 20 °C. But the further increase in the temperature of the contact interaction of up to 300 °C does not cause noticeable differences in the instantaneous stress state compared to those obtained at lower *T* values.

The σ_x compression component at *T* = 20 °C at a distance of 5 mm from SL reaches the values from $0.54\sigma_y$ on the outer to $0.27\sigma_y$ on the back surface of the plate (Figure 4, *a*). The compression σ_x stresses at a distance of 5 mm from SL reach the values from $0.79\sigma_y$ on the outer to $0.42\sigma_y$ on the back surfaces of AMg6 alloy at *T* = 150 °C (Figure 4, *b*). Instantaneous stresses reach the maximum values at 300 °C. Thus, the σ_x compression component at a distance of 5 mm from SL reaches the values from $1.4\sigma_y$ on the outer to $0.94\sigma_y$ on the back surfaces of AMg6 alloy at *T* = 300 °C (Figure 4, *c*).

Figure 5 shows the results of computation of the instantaneous distributions of σ_x in the plates δ = 8 mm, which differ significantly from the stress states of the plates δ = 2 and 4 mm. It can be seen that both along SL, as well as at a distance of 5 mm from it, σ_x transfer from compression stresses on the outer surface to tensile stresses on the back one in the entire investigated temperature range.

Thus, at *T* = 20 °C, the values of σ_x along SL change from $0.48\sigma_y$ compression on the outer surface to σ_y tensile on the opposite one, and at a distance of 5 mm from SL — from $0.46\sigma_y$ compression on the outer to $0.6\sigma_y$ tensile on the opposite one (Figure 5, *a*). At *T* = 150 °C, the values of σ_x along SL change from $0.64\sigma_y$ compression on the outer surface to $1.2\sigma_y$ tensile on the opposite one, and at a distance of 5 mm from SL — from $0.9\sigma_y$ compression on the outer surface to $0.76\sigma_y$ tensile on the opposite one (Figure 5, *b*).

When *T* grows to 300 °C, the metal undergoes intense elastic-plastic flow during EDT, which can be explained by high-temperature heating of a significant volume (compared to δ = 2–4 mm) of metal in the contact zone. Thus, the values of compression σ_x on the contact surface (point *B*) and tension on the back surface (point *C*) of the plate along SL and at a distance of 5 mm from SL exceed σ_y (Figure 5, *c*).

Table 2 presents the generalized results of modeling RSS of the σ_x component along SL and at a distance of 5 mm from SL for the plates δ = 2–8 mm after EDT at different T. The stress values are given in relation to $\sigma_y = f(T)$ (Table 1), which correspond to *T* value, for which the contact interaction was calculated. The lines 1, 4, and 7 show the values of the

Table 2. Relative values of RSS σ_x component in the butt joints of AMg6 alloy δ = 2; 4 and 8 mm after their EDT under conditions of heating to *T* = 20, 150 and 300 °C

Number	δ, mm	*T*, °C	Values of $\sigma_x \times \sigma_y$ at the points along the line *B–C*			Values of $\sigma_x \times \sigma_y$ at the points at a distance of 5 mm from the line *B–C*		
			B	δ/2	*C*	*B*	δ/2	*C*
1	2	RSS at 20 °C*	–1	–1	–1	–1	–0.5	–0.4
2		RSS at 20 °C* after EDT at *T* = 150 °C	–1.2	–1.26	–1.23	–1.16	–0.66	–0.5
3		RSS at 20 °C* after EDT at *T* = 300 °C	–0.43	–0.45	–0.46	–0.4	–0.32	–0.4
4	4	RSS at 20 °C*	–0.88	–1.0	–0.72	–0.54	–0.2	–0.27
5		RSS at 20 °C* after EDT at *T* = 150 °C	–0.93	–1.0	–0.83	–0.73	–0.34	–0.43
6		RSS at 20 °C* after EDT at *T* = 300 °C	–0.44	–0.5	–0.54	–0.49	–0.38	–0.41
7	8	RSS at 20 °C*	–0.48	–0.4	1	–0.46	0.2	0.6
8		RSS at 20 °C* after EDT at *T* = 150 °C	–0.59	–0.53	1.15	–0.83	0.17	0.72
9		RSS at 20 °C* after EDT at *T* = 300 °C	–0.7	–0.66	1.0	–1.2	0	0.5

*RSS values are given in relation to $\sigma_y = f(T)$ in Table 1.

σ_x RSS component of the plates, respectively, δ = 2, 4, and 8 mm after EDT at T = 20 °C. In the lines 2, 5 and 8, residual σ_x for δ = 2, 4 and 8 mm after cooling from T = 150 to 20 °C and in 3, 6 and 9 similarly after cooling from T = 300 to T = 20 °C.

When comparing the data of the lines 1, 4, and 7 for T = 20 °C, the lines 2, 5, and 8 for T = 150 °C, and the lines 3, 6, and 9 for 300 °C, it can be seen that EDT of the plates δ = 2–4 mm at T = 20–300 °C along SL promotes the formation of compression σ_x. However, the effect of treatment is significantly reduced when δ grows to 8 mm, which contributes to the reduction of peak values of compression stresses and transition from compression on the contact (at the point *B*) to tensile on the back (point *C*) surfaces.

For the section "5 mm from SL" the pattern is somewhat different. For example, when δ grows from 2 to 4 mm, the values of compression σ_x decrease almost by half from the outer surface — point *B* to the back one — point *C*. Thus, with an increase in δ, the effect of EDT on the metal of welded joint near the fusion line decreases. An increase in δ to 8 mm determines a decrease in the peak compression σ_x stresses compared to δ = 2–4 mm and the formation of tensile stresses on the sections δ/2 and on the back surface at the point *C*.

Summarizing the abovementioned data, it should be noted that for EDT application when δ = 2–4 mm, the optimal T value is 150 °C, at which AMg6 alloy does not significantly lose its elastic properties (see Table 1).

However, for δ = 8 mm, the action of T does not have such a noticeable effect on the efficiency of EDT for RSS correction (at a set V_0 value), as for δ = 2–4 mm. When comparing the lines 7, 8 and 9, it is possible to see a slight difference in σ_x values, that were obtained as a result of EDT at T = 20–300 °C for δ = 2–4 mm.

Based on the results of Figures 3–5 and Table 2, it should be noted that at a set vertical velocity V_0 of the electrode-indenter (Figure 1), one-sided EDT contributes to the formation of compression RSS on both surfaces of the welded joints of AMg6 alloy plates δ = 2–4 mm in contrast to δ = 8 mm, where tensile stresses are formed on the back surface. Thus, at V_0 = 5 m/s, it is advisable to carry out double-sided EDT of AMg6 alloy plates δ = 8 mm to obtain compression RSS on both sides of the welded joints.

The obtained results can be explained by the fact that EDT at T = 150 °C initiates the formation of higher relative instantaneous σ_x stresses compared to stresses at T = 20 °C. This contributes to the formation of higher compression RSS when the plate cools down compared to RSS after EDT at T = 20 °C. The given results can be explained by the fact that at T = 150 °C, AMg6 alloy does not yet lose its elastic properties, and thermal exposure additionally stimulates stress relaxation mechanisms, which is confirmed by the data [7]. However, during EDT at T = 300 °C, instantaneous stresses, the values of which are lower than at T = 150 °C, respectively, contribute to the formation of lower compressive RSS (compared to RSS after EDT at T = 150 °C).

The presented computational results showed that EDT of the welded joint metal δ = 2–8 mm of AMg6 alloy, performed at T = 150 °C (which models treatment in a single process in simultaneously with fusion welding), is more efficient compared to EDT at T = 300 °C or with separate EDT after welding (which corresponds to EDT at T = 20 °C). The efficiency of EDT is determined by the formation of higher compression RSS values of the produced welded joint. At the same time, to form compression RSS across the thickness of welded joints δ = 2–4 mm, it is enough to perform one-sided EDT (at a set V_0 value) and double-sided EDT for δ = 8 mm.

CONCLUSIONS

1. On the basis of the developed mathematical model of the dynamic interaction of the electrode-indenter with a butt welded joint of AMg6 alloy δ = 2–8 mm, a numerical evaluation of the effect of δ on the kinetics of stresses and RSS of plates as a result of electrodynamic treatment (EDT) at elevated temperatures was carried out.

2. According to the results of computations, it was proved that the use of EDT of AMg6 alloy weld metal δ = 2–8 mm, performed at T = 150 °C (condition for modelling EDT in a single process simultaneously with fusion welding), contributes to the formation of higher compression RSS stresses compared to EDT at T = 300 °C or separate EDT after welding at T = 20 °C.

3. At the same time, to form compression RSS across the thickness of welded joints δ = 2–4 mm, it is sufficient to perform one-sided EDT (at a set value of contact velocity V_0), and double-sided for δ = 8 mm.

REFERENCES

1. Madi, Y., Besson, J. (2014) *Effect of residual stresses on brittle fracture. Mat. ECRS-9.* UTT, Troyes, France.
2. (2022) *Welding and technical diagnostics for the recovery of the economy of Ukraine*: Abstr. of Reports Sci. Conf. Kyiv, IAW.
3. Lobanov, L.M., Pashchin, N.A., Mikhodui, O.L., Sidorenko, Y.M. (2018) Electric pulse component effect on the stress state of AMg6 aluminum alloy welded joints under electrodynamic treatment. *Strength of Materials*, 50(**2**), 246–253. DOI: https://doi.org/10.1007/s11223-017-9862-8
4. Sydorenko, Y.M., Pashchyn, M.O., Mikhodui, O.L. et al. (2020) Effect of pulse current on residual stresses in AMg6

aluminum alloy in electrodynamic treatment. *Strength of Materials*, 52(**5**), 731–737. DOI: https://doi.org/10.1007/s11223-020-00226-2
5. Conrad, H., Sprecher, A. (1989) *The electroplastic effect in metals*. Ed. by F.R.N. Nabarro. Elsevier Sci. Publ. B.V., Dislocations in Solids, 500–529.
6. Shao, Quan, Kang, Jiajie, Xing, Zhiguo et al. (2019) Effect of pulsed magnetic field treatment on the residual stress of 20Cr2Ni4A steel. *J. of Magnetizm and Magnetic Materials*, **476**, 218–224.
7. Stepanov, G.V., Babutskii, A.I., Mameev, I.A. (2004) High-density pulse current-induced unsteady stress-strain state in a long rod. *Strength of Materials*, **36**, 377–381. DOI: https://doi.org/10.1023/B:STOM.0000041538.10830.34
8. Lobanov, L.M., Pashchyn, M.O., Mikhodui, O.L. et al. (2022) Stress-strain state of welded joints of AMg6 alloy after electrodynamic treatment during welding. *Strength of Materials*, 54(**6**), 983–996. DOI: https://doi.org/10.1007/s11223-023-00474-y
9. Lobanov, L.M., Pashchin, N.A., Mikhodui, O.L. (2012) Efficiency of electrodynamic treatment of welded joints of AMg6 alloy of different thickness. *The Paton Welding J.*, **3**, 6–10.
10. http://www.ansys.com/.
11. Masubuchi, K. (1980) *Analysis of welded structures.* Pergamon Press, Oxford, United Kingdom.

ORCID
L.M. Lobanov: 0000-0001-9296-2335,
M.O. Pashchyn: 0000-0002-2201-5137,
O.L. Mikhodui: 0000-0001-6660-7540,
N.L. Todorovych: 0000-0002-3872-5790,
Yu.M. Sydorenko: 0000-0001-8780-9459,
P.R. Ustymenko: 0000-0002-5318-2675

CONFLICT OF INTEREST
The Authors declare no conflict of interest

CORRESPONDING AUTHOR
M.O. Pashchyn
E.O. Paton Electric Welding Institute of the NASU
11 Kazymyr Malevych Str., 03150, Kyiv, Ukraine.
E-mail: svarka2000@ukr.net

SUGGESTED CITATION
L.M. Lobanov, M.O. Pashchyn, O.L. Mikhodui, N.L. Todorovych, Yu.M. Sydorenko, P.R. Ustymenko (2024) Computational evaluation of the influence of the thickness of welded joints of AMg6 alloy on their stress-strain state after electrodynamic treatment in the process of welding. *The Paton Welding J.*, **4**, 11–17.

JOURNAL HOME PAGE
https://patonpublishinghouse.com/eng/journals/tpwj

Received: 13.11.2023
Received in revised form: 09.02.2024
Accepted: 07.05.2024